Communication: Observation of dipole-bound state and high-resolution photoelectron imaging of cold acetate anions

Dao-Ling Huang, Guo-Zhu Zhu, and Lai-Sheng Wang

Citation: The Journal of Chemical Physics **142**, 091103 (2015); doi: 10.1063/1.4913924
View online: http://dx.doi.org/10.1063/1.4913924
View Table of Contents: http://scitation.aip.org/content/aip/journal/jcp/142/9?ver=pdfcov
Published by the AIP Publishing

Communication: Observation of dipole-bound state and high-resolution photoelectron imaging of cold acetate anions

Dao-Ling Huang, Guo-Zhu Zhu, and Lai-Sheng Wang[a)]
Department of Chemistry, Brown University, Providence, Rhode Island 02912, USA

(Received 23 January 2015; accepted 19 February 2015; published online 4 March 2015)

We report the observation of a dipole-bound state and a high-resolution photoelectron imaging study of cryogenically cooled acetate anions (CH_3COO^-). Both high-resolution non-resonant and resonant photoelectron spectra via the dipole-bound state of CH_3COO^- are obtained. The binding energy of the dipole-bound state relative to the detachment threshold is determined to be 53 ± 8 cm^{-1}. The electron affinity of the CH_3COO• neutral radical is measured accurately as $26\,236 \pm 8$ cm^{-1} (3.2528 ± 0.0010 eV) using high-resolution photoelectron imaging. This accurate electron affinity is validated by observation of autodetachment from two vibrational levels of the dipole-bound state of CH_3COO^-. Excitation spectra to the dipole-bound states yield rotational profiles, allowing the rotational temperature of the trapped CH_3COO^- anions to be evaluated. © *2015 AIP Publishing LLC.* [http://dx.doi.org/10.1063/1.4913924]

The acetyloxyl radical (CH_3COO•) is a prototypical carboxyl radical that plays key roles in a wide range of organic syntheses, atmospheric, and combustion chemistry.[1–4] CH_3COO• is a common organic reaction intermediate and is believed to be an intermediate in the bimolecular reactions of $CH_3O + CO$.[3–5] The structure and thermodynamic properties of CH_3COO• are important for understanding reaction mechanisms involving higher carboxyl radicals. However, this seemingly simple radical has posed considerable challenge to both experimental and theoretical studies because of the existence of several low-lying electronic states and symmetry breaking issues.[6–9]

Anion photoelectron spectroscopy (PES) is a powerful technique for the study of the electronic structures of short-lived neutral radicals. However, the spectral resolution of PES is usually limited to several meV, preventing the observation of low frequency vibrations. In addition, photodetachment processes are governed by the Franck-Condon principle. For detachment transitions with very weak Franck-Condon factors, i.e., large geometry changes between the anion and the neutral final state, the capability of anion PES is limited.[10] It has been shown that anion cooling is critical to accurately determining electron affinities (EAs) of neutral radicals, because vibrational hot bands are completely eliminated, which allows direct measurement of the 0_0^0 transition from the corresponding anions.[11–13] The EA of CH_3COO• is an important thermodynamic property and has been studied with a variety of techniques.[14–18] However, the large geometry change between the acetate anion and CH_3COO• results in a very weak Franck-Condon factor for the 0_0^0 transition,[7] making it difficult to observe the neutral vibrational ground state. In most cases, only an upper limit of the EA was estimated. The most accurate EA was reported to be 3.250 ± 0.010 eV from a combined low-temperature PES and *ab initio* study.[19] A vibrational progression with a spacing of 545 ± 40 cm^{-1} was partially resolved (see Fig. 1(d)). Nevertheless, the assignment of the first weak peak to be the 0_0^0 transition instead of an upper limit was mainly based on theoretical calculations.[19]

The simpler HCOO• radical has been better characterized using anion PES.[20] The vibronic structure of HCOO• has been reported via slow electron velocity-map imaging (SEVI) spectroscopy, giving rise to an accurate EA of 3.4961 ± 0.0010 eV.[21] Photoelectrons corresponding to the ground state ($^2A_1$) of HCOO• have *p*-wave character and those corresponding to the $^2B_2$ excited state, which lies only 218 ± 121 cm^{-1} higher, have *s*-wave character.[21] While information about photoelectron angular distribution (PAD) of CH_3COO• is lacking, *ab inito* calculations indicated that the symmetry of the ground state of CH_3COO• is different from that for HCOO•, that is, the ground state of CH_3COO• is $^2A''$ (B_2), with a $^2A'$ (A') low-lying excited state ~0.1–0.2 eV higher in energy.[7]

Molecules with sufficient dipole moments can bind an electron[22–25] and form dipole-bound anions.[26–29] Resonances observed in photodetachment experiments provided the first evidence for excited dipole-bound states (DBSs) near detachment thresholds of anions.[30–32] High resolution photodetachment spectroscopy was obtained via rotational autodetachment from DBSs.[33–35] However, the studies of autodetachment dynamics of DBSs were hindered by congested spectra at room temperature. Recently, we directly observed mode-specific vibrational autodetachment from DBSs of cold phenoxide anions,[36] which were cooled in a temperature-controlled ion trap to eliminate vibrational hot bands and minimize rotational broadening. The $\Delta v = -1$ vibrational propensity rule, which was initially developed for autoionzation from Rydberg states[37] and extended to autodetachment,[38] was directly observed. More importantly, the vibrational frequencies of the DBS were measured to be the same as the neutral, suggesting the extra electron in the DBS of the anion has very little effect on the neutral core, analogous to a Rydberg state.

a)Email: Lai-Sheng_Wang@brown.edu

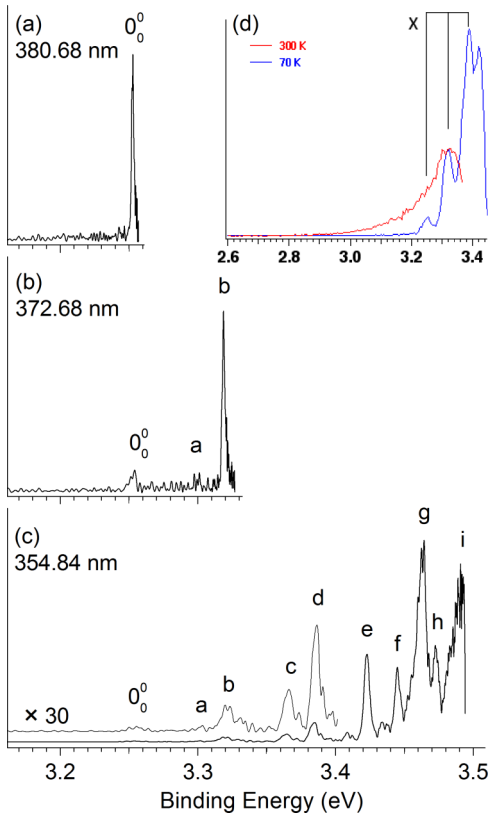

FIG. 1. High-resolution photoelectron spectra of CH_3COO^- at (a) 380.38 nm, (b) 372.68 nm, and (c) 354.84 nm using photoelectron imaging (see Fig. S1 for the images). The previous low resolution photoelectron spectra at 354.84 nm and two temperatures[19] are reproduced for comparison in (d).

Subsequently, vibrational spectroscopy of the dehydrogenated uracil radical was obtained via autodetachment from a DBS of the anion;[39] a total of 46 resonant peaks were observed and 21 out of 27 fundamental vibrational modes of the uracil radical were reported.

Preliminary calculations suggest that the CH_3COO• radical should have a dipole moment of ~3.5 D,[40] which is large enough to support a DBS. Here, we report the direct observation of a DBS in CH_3COO^- with a binding energy (BE) of only 53 ± 8 cm^{-1} relative to the detachment threshold. Autodetachment via two vibrational levels of the excited DBS of CH_3COO^- is observed in both photodetachment spectra by monitoring the total electron yield and resonant PE images. The EA of CH_3COO• is measured accurately using high-resolution PE imaging to be 26 236 ± 8 cm^{-1} (3.2528 ± 0.0010 eV) and is validated by vibrational autodetachment that reaches exclusively to the vibrational ground state of CH_3COO•. Excitation spectra to the DBS result in rotational profiles, allowing the rotational temperature of CH_3COO^- to be evaluated.

Our high-resolution PE imaging apparatus[41] is equipped with an electrospray ionization (ESI) source,[42] a temperature-controlled cryogenic ion trap,[11–13] and a time-of-flight mass spectrometer. This apparatus is an improved version based on our original ESI-PES system that consisted of a room-temperature ion trap and a magnetic-bottle PES analyzer.[42–45] One advantage of PE imaging is the PAD, which provides information about the nature of the occupied molecular orbital from which the electron is ejected.[46,47] The acetate anions were generated by electrospray of 1 mM solution of CH_3COONa dissolved in a mixed CH_3OH/H_2O solvent (9:1 volume ratio). After passing through two radio-frequency (RF) quadrupole ion guides and one RF-only octopole ion guide, the anions were loaded into a cryogenically cooled Paul trap in a more compact linear configuration,[13] compared with our first generation cold ion trap.[12] The lowest temperature that the current cold trap can achieve is 4.4 K, measured by a thermal couple off the outer wall of the Paul trap. The anions were accumulated and cooled via collisions with a He/H_2 (4:1 volume ratio) buffer gas (~1 mTorr) in the ion trap for 0.1 s before being pulsed out into the extraction zone of a time-of-flight mass spectrometer and selected by a mass gate. The CH_3COO^- anions were focused into a co-linear velocity-map imaging lens,[41] where anions were photodetached by a linearly polarized laser beam. Photoelectrons were projected onto a position-sensitive detector with a pair of 75-mm diameter micro-channel plates coupled to a phosphor screen and captured by a charge-coupled device camera. The recorded PE images were inverse-Abel transformed to obtain 3-dimensional photoelectron distributions. This reconstruction was carried out using both pBASEX[48] and BASEX,[49] which gave similar results.

Two photodetachment laser systems were used in the current study: a Nd:YAG laser and a Nd:YAG pumped dye laser. The experiments reported in the current work were all performed by operating the ion trap at 4.4 K to achieve the best cooling.[50] The velocity-map imaging apparatus was calibrated with the PE images of Au^- at several photon energies. The kinetic energy (KE) resolution achieved was 3.8 cm^{-1} for 55 cm^{-1} electrons and about 1.5% (ΔKE/KE) for KE above 1 eV.

Fig. 1 shows the high-resolution PE spectra of CH_3COO^- at three different photon energies. The corresponding PE images are given in Fig. S1 in the supplementary material.[51] Fig. 1(d) reproduces the earlier PE spectra at 354.84 nm, obtained by the magnetic-bottle PE analyzer,[19] for comparison. The spectra in Figs. 1(d) and 1(c) were taken at the same photon energy. Due to the spectral cutoff of the magnetic-bottle analyzer, the spectrum in Fig. 1(d) was only observed up to ~3.4 eV binding energy (the last peak beyond 3.4 eV was an artifact due to the cutoff). The PE spectrum up to 3.4 eV in Fig. 1(c) was expanded by 30 times to make the 0_0^0, *a*–*d* features discernable. It is readily seen that the resolution is significantly improved in the current experiment. Fig. 1(d) shows only three peaks between 3.2–3.4 eV and the first weak peak was assigned as the 0_0^0 transition, that gave the EA of 3.250 ± 0.010 eV reported previously.[19] In the same 3.2–3.4 eV photon energy range, five peaks were resolved in Fig. 1(c) (0_0^0, *a*–*d*). Under active cooling, the vibrational hot bands were completely eliminated. The first extremely weak peak assigned to the 0_0^0 transition in Fig. 1(c) is consistent with that in Fig. 1(d). Higher resolution spectra were taken at 372.68 nm (Fig. 1(b)) and 380.68 nm (Fig. 1(a)) to better resolve the first three peaks, 0_0^0, *a*, and *b*.

In Fig. 1(a), the 0_0^0 peak width was measured to be 15 cm^{-1} at about 30 cm^{-1} kinetic energy, suggesting severe rotational broadening. We determined the EA of CH_3COO•

to be 26236 ± 8 cm^{-1} (3.2528 ± 0.0010 eV) at the top of the 0_0^0 peak. The peaks *a* and *b* in Fig. 1(b) have a spacing of about 385 cm^{-1} and 536 cm^{-1} from the 0_0^0 peak, respectively. By comparison with the calculated vibrational frequencies listed in Table S1 in the supplementary material,[51] the *a* and *b* peaks were assigned to two fundamental vibrational modes, 14_0^1 and 8_0^1, respectively. The reason why the strong *b* peak was assigned to be 8_0^1 instead of 9_0^1 is that v_8 represents the OCO bending mode, which should be very active upon one-electron removal from CH_3COO^- because there is a large ∠O-C-O bond angle change associated with this detachment transition.[19] The v_9 mode is a C-C in-plane wagging mode,[40] which was expected to have a weak Franck-Condon factor.

However, the five features at low binding energies are very weak relative to the peaks *e*–*i* resolved beyond 3.4 eV (Fig. 1(c)). All the peak positions, shifts from the 0_0^0 peak, PADs, and assignments for the peaks *a*–*d*, are given in Table S2 in the supplementary material.[51] It is noted that peaks *g* and *i* are much broader than peaks *e*, *f*, and *h*, indicating that several close-lying transitions may contribute to these two peaks. The PAD can be difficult to interpret for complex molecules,[47] but still can provide valuable electronic information. The PADs show that features 0_0^0, *b*–*d* all have *s*-wave character while peaks *e*–*i* all have *p*-wave character (Fig. S1), suggesting that these two sets of peaks correspond to two different electronic states. The weak intensity of the *a* peak prevents its PAD to be measured. Thus, the origin of the first excited electronic state of CH_3COO• is expected to be the *e* peak and it is 1371 cm^{-1} higher than that of the neutral ground state, in good agreement with the calculated 0.1–0.2 eV excitation energy.[7] The *s*-wave PAD of the 0_0^0 peak indicates that the highest occupied molecular orbital of CH_3COO^- should be a *p*-type orbital, which is quite different from what was observed for $HCOO^-$: the PAD of the 0_0^0 peak of HCOO• has *p*-wave character.[21] Moreover, the observed *p*-wave PAD of the excited state of CH_3COO^- is also different from that reported for the first excited electronic state of HCOO•. Our observed PAD of the PE images of CH_3COO^- is consistent with the theoretical predication that the ground state of CH_3COO• is $^2A''$ (B_2) with the $^2A'$ (A') low-lying excited state.[7]

Fig. 2 displays the photodetachment spectrum of CH_3COO^- in the photon energy range 373.65–375.25 nm by monitoring the total electron yield to search for DBSs in the vicinity of the 14_0^1 and 8_0^1 levels of CH_3COO•. As seen from Table S2, the measured fundamental frequencies for the v_{14} and v_8 modes (peaks *a* and *b* in Fig. 1) are 387 and 536 cm^{-1}, respectively. We expected that transitions to the $14_0'^1$ and $8_0'^1$ vibrational levels of the DBS should occur near the 14_0^1 and 8_0^1 levels of CH_3COO•, because the binding energy of the DBS was expected to be small.[36,39] Since the photodetachment spectrum was taken over ~300–530 cm^{-1} above the detachment threshold, the overall baseline represents the direct photodetachment from the electronic ground state of CH_3COO^- to that of CH_3COO•. In addition to the weak direct detachment signals, two peaks were observed and labeled as 1 and 2, which must be due to autodetachment by resonant excitation to an electronic excited state of CH_3COO^-. The energy difference between features 1 and 2 is 150 cm^{-1}, identical to that between peaks *a* and *b* in Fig. 1, i.e., the

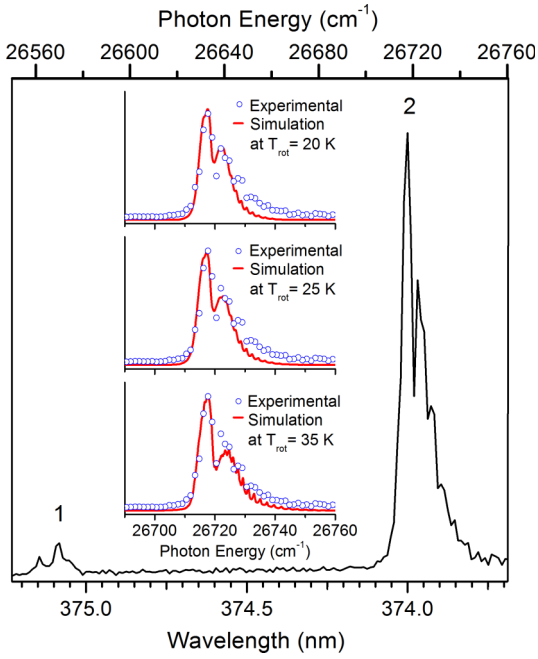

FIG. 2. Photodetachment spectrum of CH_3COO^- in the photon energy range from 373.65 to 375.25 nm in the vicinity of the 14_0^1 and 8_0^1 levels of neutral CH_3COO•, i.e., near the binding energies of the *a* and *b* peaks in Fig. 1(b). Peaks 1 and 2 represent autodetachment via resonant excitation to the $14'^1_0$ and $8'^1_0$ vibrational levels of the dipole-bound state. The rotational profiles suggest that peak 1 is an *a*-type transition and peak 2 is a *b*-type transition. The inset shows comparison between the experimental spectrum of peak 2 and simulated rotational profiles at three rotational temperatures (T_{rot}).

excited state of CH_3COO^- has vibrational levels similar to the neutral. This is the main character of DBSs of anions observed previously.[36,39] Hence, features 1 and 2 are due to the $14_0'^1$ and $8_0'^1$ vibrational levels, respectively, of the excited DBS of CH_3COO^-, as we expected.

Considerable rotational broadening was observed in the two vibrational peaks 1 (*a*-type) and 2 (*b*-type). To evaluate the rotational temperature (T_{rot}), we used the PGOPHER program[52] to simulate the rotation profile for the more intense v_8 band, as shown in the inset of Fig. 2 at three T_{rot}: 20, 25, and 35 K. Both the rising edge and the splitting in the experimental spectrum are well reproduced by the simulations at all three T_{rot}, though the relative intensity of the higher energy side varies with T_{rot}. Therefore, we estimated that the actual T_{rot} of the trapped CH_3COO^- anions should be in the range of 20–35 K, which is consistent with the 35 K rotational temperature estimated previously for the trapped deprotonated uracil anions.[39]

Fig. 3 shows the resonant PE images and spectra of CH_3COO^- measured at 376.36 and 374.27 nm, when the detachment laser was tuned to the positions of 1 and 2 in Fig. 2, respectively. The PE signals should be dominated by vibrational autodetachment from the DBS of CH_3COO^-. According to the $\Delta v = -1$ propensity rule, the neutral final state via autodetachment from the $14_0'^1$ and $8_0'^1$ levels of the DBS should be the ground vibrational state of the neutral, as schematically shown in Fig. 4. The observed binding energies of the main peaks in Fig. 3 correspond to the 0_0^0 peak in Fig. 1, confirming unequivocally the assignment of the 0_0^0 peak in the

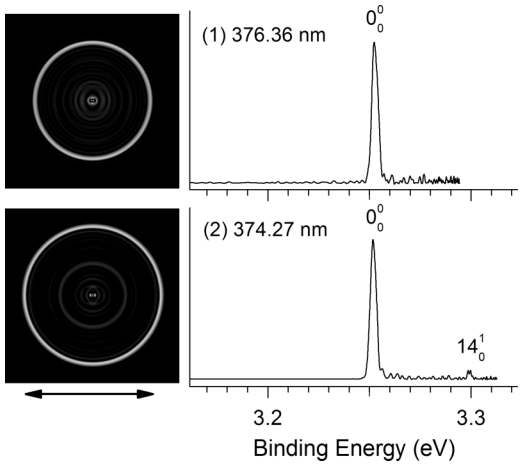

FIG. 3. High-resolution resonant photoelectron spectra of CH_3COO^- at two photon energies. The images were reconstructed using pBasex[48] and the double arrow below the images indicates the laser polarization. The two detachment photon energies correspond to peaks 1 and 2 in Fig. 2.

non-resonant PE spectra. Note that the intensity of the 0^0_0 peak in Fig. 3 is completely non-Franck-Condon.

As shown in Fig. 4, we can evaluate the excitation energy to the ground vibrational state of the DBS (26 183 cm^{-1}) and its binding energy (53 cm^{-1}) relative to the detachment threshold, using the EA of CH_3COO•, the vibrational frequencies of the ν_{14} and ν_8 modes, and the excitation energies to the $14'^1_0$ and $8'^1_0$ levels of the DBS. The evaluated excitation energy (26 183 cm^{-1}) to the vibrational ground state of the DBS corresponds to a wavelength of 381.92 nm. When we scanned our dye laser around this region, we indeed observed a weak resonant two-photon detachment

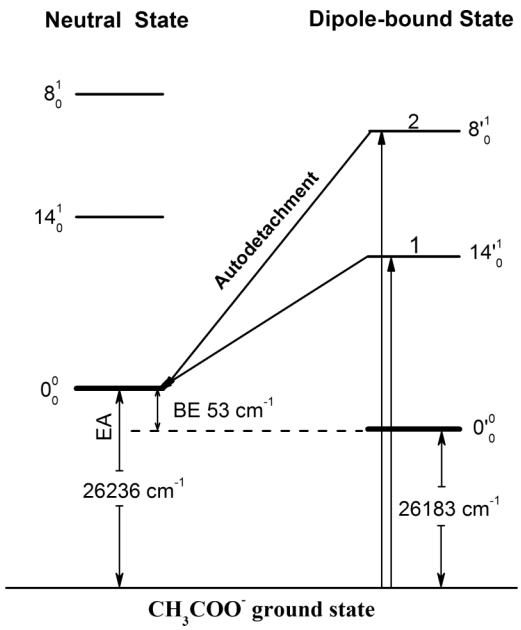

FIG. 4. Schematic energy levels for the transitions from the anion ground state to the vibrationally excited dipole-bound states of CH_3COO^- and the autodetachment from the dipole-bound states to the neutral ground state of CH_3COO•. The labels 1 and 2 correspond to the resonant peaks observed in Fig. 2. The EA of CH_3COO• and the BE of the dipole-bound state are indicated.

peak, which is just below the detachment threshold, as shown in Fig. S2 in the supplementary material.[51] Because of the weak Franck-Condon factor for the 0^0_0 transition, the electron signals were very weak near the detachment threshold of 381.15 nm (Fig. S2(b)). Fig. S2(a) shows a better two-photon detachment spectrum for the ground vibrational state of the DBS at 381.92 nm by averaging much longer time than the broad scan in Fig. S2(b). The rotational profile for this spectrum is similar to that of peak 2 in Fig. 2.

In conclusion, we have observed a dipole-bound state for CH_3COO^- and obtained an accurate electron affinity for CH_3COO• as 26236 ± 8 cm^{-1} (3.2528 ± 0.0010 eV) using high-resolution photoelectron imaging and photodetachment experiment of cold acetate anions. The detachment transition to the vibrational ground state of CH_3COO• is unequivocally established from the observation of autodetachment from two vibrational levels of the dipole-bound state. The fundamental vibrational frequencies of the ν_8 and ν_{14} modes of CH_3COO• are measured as 536(8) cm^{-1} and 387(8) cm^{-1}, respectively. The binding energy of the dipole-bound state is measured to be 53(8) cm^{-1} relative to the detachment threshold. Rotational profiles are observed in the excitation spectra to the vibrational levels of the dipole-bound state, yielding a rotational temperature of ~20–35 K for the acetate anions.

ACKNOWLEDGMENTS

This work was supported by the National Science Foundation (No. CHE-1263745).

[1]L. Herk, M. Feld, and M. Szwarc, J. Am. Chem. Soc. **83**, 2998 (1961).
[2]P. S. Skell and D. D. May, J. Am. Chem. Soc. **105**, 3999 (1983).
[3]B. S. Wang, H. Hou, and Y. S. Gu, J. Phys. Chem. A **103**, 8021 (1999).
[4]Z. Y. Zhou, X. L. Cheng, X. M. Zhou, and H. Fu, Chem. Phys. Lett. **353**, 281 (2002).
[5]Y. Z. Zhou, S. Li, Q. S. Li, and S. W. Zhang, J. Mol. Struct.: THEOCHEM **854**, 40 (2008).
[6]S. D. Peyerimhoff, P. S. Skell, D. D. May, and R. J. Buenker, J. Am. Chem. Soc. **104**, 4515 (1982).
[7]A. Rauk, D. Yu, and D. A. Armstrong, J. Am. Chem. Soc. **116**, 8222 (1994).
[8]E. Sicilia, F. P. Dimaio, and N. Russo, J. Phys. Chem. **97**, 528 (1993).
[9]M. Kieninger, O. N. Ventura, and S. Suhai, Int. J. Quantum Chem. **70**, 253 (1998).
[10]P. G. Wenthold, D. A. Hrovat, W. T. Borden, and W. C. Lineberger, Science **272**, 1456 (1996).
[11]X. B. Wang, H. K. Woo, and L. S. Wang, J. Chem. Phys. **123**, 051106 (2005).
[12]X. B. Wang and L. S. Wang, Rev. Sci. Instrum. **79**, 073108 (2008).
[13]P. D. Dau, H. T. Liu, D. L. Huang, and L. S. Wang, J. Chem. Phys. **137**, 116101 (2012).
[14]Z. Lu and R. E. Continetti, J. Phys. Chem. A **108**, 9962 (2004).
[15]M. V. Muftakhov, Y. V. Vasil'ev, and V. A. Mazunov, Rapid Commun. Mass Spectrom. **13**, 1104 (1999).
[16]R. Yamdagni and P. Kebarle, Ber. Bunsen-Ges. Phys. Chem. **78**, 181 (1974).
[17]W. E. Wentworth, E. Chen, and J. C. Steelhammer, J. Phys. Chem. **72**, 2671 (1968).
[18]L. S. Wang, C. F. Ding, X. B. Wang, and J. B. Nicholas, Phys. Rev. Lett. **81**, 2667 (1998).
[19]X. B. Wang, H. K. Woo, L. S. Wang, B. Minofar, and P. Jungwirth, J. Phys. Chem. A **110**, 5047 (2006).
[20]E. H. Kim, S. E. Bradforth, D. W. Arnold, R. B. Metz, and D. M. Neumark, J. Chem. Phys. **103**, 7801 (1995).
[21]E. Garand, K. Klein, J. F. Stanton, J. Zhou, T. I. Yacovitch, and D. M. Neumark, J. Phys. Chem. A **114**, 1374 (2010).
[22]W. R. Garrett, Chem. Phys. Lett. **5**, 393 (1970).
[23]W. R. Garrett, Phys. Rev. A **3**, 961 (1971).
[24]K. Rohr and F. Linder, J. Phys. B: At. Mol. Phys. **9**, 2521 (1976).
[25]J. E. Turner, Am. J. Phys. **45**, 758 (1977).

[26]J. A. Stockdale, F. J. Davis, R. N. Compton, and C. E. Klots, J. Chem. Phys. **60**, 4279 (1974).
[27]H. Haberland, C. Ludewigt, H. G. Schindler, and D. R. Worsnop, J. Chem. Phys. **81**, 3742 (1984).
[28]C. Desfrancois, B. Baillon, J. P. Schermann, S. T. Arnold, J. H. Hendricks, and K. H. Bowen, Phys. Rev. Lett. **72**, 48 (1994).
[29]N. I. Hammer, R. J. Hinde, R. N. Compton, K. Diri, K. D. Jordan, D. Radisic, S. T. Stokes, and K. H. Bowen, J. Chem. Phys. **120**, 685 (2004).
[30]A. H. Zimmerman and J. I. Brauman, J. Chem. Phys. **66**, 5823 (1977).
[31]R. L. Jackson, A. H. Zimmerman, and J. I. Brauman, J. Chem. Phys. **71**, 2088 (1979).
[32]R. L. Jackson, P. C. Hiberty, and J. I. Brauman, J. Chem. Phys. **74**, 3705 (1981).
[33]K. R. Lykke, R. D. Mead, and W. C. Lineberger, Phys. Rev. Lett. **52**, 2221 (1984).
[34]K. R. Lykke, D. M. Neumark, T. Andersen, V. J. Trapa, and W. C. Lineberger, J. Chem. Phys. **87**, 6842 (1987).
[35]K. Yokoyama, G. W. Leach, J. B. Kim, and W. C. Lineberger, J. Chem. Phys. **105**, 10696 (1996).
[36]H. T. Liu, C. G. Ning, D. L. Huang, P. D. Dau, and L. S. Wang, Angew. Chem., Int. Ed. **52**, 8976 (2013).
[37]R. S. Berry, J. Chem. Phys. **45**, 1228 (1966).
[38]J. Simons, J. Am. Chem. Soc. **103**, 3971 (1981).
[39]H. T. Liu, C. G. Ning, D. L. Huang, and L. S. Wang, Angew. Chem., Int. Ed. **53**, 2464 (2014).
[40]The dipole moment and the frequencies of $CH_3COO\bullet$ were calculated at the B3LYP/6–31+G(d,p) level of theory.
[41]I. Leon, Z. Yang, H. T. Liu, and L. S. Wang, Rev. Sci. Instrum. **85**, 083106 (2014).
[42]L. S. Wang, C. F. Ding, X. B. Wang, and S. E. Barlow, Rev. Sci. Instrum. **70**, 1957 (1999).
[43]H. T. Liu, Y. L. Wang, X. G. Xiong, P. D. Dau, Z. A. Piazza, D. L. Huang, C. Q. Xu, J. Li, and L. S. Wang, Chem. Sci. **3**, 3286 (2012).
[44]P. D. Dau, J. Su, H. T. Liu, J. B. Liu, D. L. Huang, J. Li, and L. S. Wang, Chem. Sci. **3**, 1137 (2012).
[45]P. D. Dau, J. Su, H. T. Liu, D. L. Huang, J. Li, and L. S. Wang, J. Chem. Phys. **137**, 064315 (2012).
[46]D. M. Neumark, J. Phys. Chem. A **112**, 13287 (2008).
[47]E. R. Grumbling and A. Sanov, J. Chem. Phys. **135**, 164302 (2011).
[48]G. A. Garcia, L. Nahon, and I. Powis, Rev. Sci. Instrum. **75**, 4989 (2004).
[49]V. Dribinski, A. Ossadtchi, V. A. Mandelshtam, and H. Reisler, Rev. Sci. Instrum. **73**, 2634 (2002).
[50]D. L. Huang, P. D. Dau, H. T. Liu, and L. S. Wang, J. Chem. Phys. **140**, 224315 (2014).
[51]See supplementary material at http://dx.doi.org/10.1063/1.4913924 for the theoretical vibrational frequencies of $CH_3COO\bullet$, the photodetachment spectra of CH_3COO^- showing the ground vibrational level of the dipole-bound state, and the photoelectron images corresponding to Fig. 1.
[52]C. M. Western, *PGOPHER, a Program for Simulating Rotational Structure* (University of Bristol, 2013) http://pgopher.chm.bris.ac.uk.